

Laser-Induced Hydrodynamic Reorientation in Hybrid Nematic Liquid Crystals

Vaharshak Hakobyan

*Department of Physics
Yerevan State University
0025 Yerevan, Armenia*

vagharshhakobyan00@gmail.com

Rafik Hakobyan

*Department of Physics
Yerevan State University
0025 Yerevan, Armenia*

rhakob@ysu.am

Corresponding Author: Vaharshak Hakobyan

Copyright © 2024 V. Hakobyan and R. Hakobyan. This is an open access article distributed under the Creative Commons Attribution License, which permits unrestricted use, distribution, and reproduction in any medium, provided the original work is properly cited.

Abstract

Liquid crystal molecules can be reoriented by weak light field. Indeed, this reorientation depends on anchoring energies, boundary conditions and also on the thickness of liquid crystal. Laser-induced hydrodynamic motions in initially hybrid oriented nematic liquid crystal have been studied theoretically under different laser power. It has been shown the reorientation of liquid crystal molecules induced by direct volume expansion mechanism for two directions of hydrodynamic flow. It has been studied the dependence of specific reorientation on anchoring energies. Hydrodynamic flow velocity gradient brings about a small increase of curvature when hydrodynamic flow velocity is directed out of the “flexible ribbon’s” curvature. The “flexible ribbon” reverses its curvature when velocity is directed into “flexible ribbon’s” curvature and when we have weak anchoring from planar boundary.

Keywords: Nematic liquid crystal, Hydrodynamics, Light-induced reorientation, Anchoring energy

1. INTRODUCTION

Light-induced reorientations in liquid crystals (LCs) were studied in many works [1-7]. It is discussed how the initial orientation of the director influences on the light-induced Frederik’s transition and analyzed several novel phenomena about interaction of light with nonuniform mesophases [8]. There are many methods for LC reorientation: electric field, magnetic field, heating etc. The laser-induced local heating of LC due to the absorption can cause phase transition if the input laser power is above threshold value. The thermal variations and phase transition can be controlled by input laser parameters and be used in phase-shifters, optical switches, [9] and femtosecond laser beam shaping [10].

The heating of LC can cause phase transitions and can be controlled. In some papers is represented the influence of the temperature gradient on the LC's director reorientation. The hydrodynamic flow of LC can appear due to the influence of heating. LC droplet starts moving with the stationary distributed velocity profile across the LC sample when thermomechanical force overcome the viscous and elastic forces [11]. It is mentioned that the characterization of the hydrodynamic flow not only depends on the temperature gradient, but also the anchoring energies [12]. There are many ways and methods to change the orientation of LC molecules. At the same time the reorientation can be controlled in a different way depends on used method. Here [13] they use Ferroelectric microplatelets and apply electric field. In this case platelets are used as a guide for LC molecules. LC reorientation is exploited to analyze the electric field generated by light irradiation in iron-doped lithium niobate crystals. The characterization of the electric field optically generated inside the LC layer is highly desirable in view of the realization of new optical devices to be integrated into optofluidic platforms [14].

If the LC is placed between two horizontal glass plates, then without any external influences it remains at rest. Nevertheless, very small absorbed light can make LC to flow. The direct volume expansion mechanism is one of the mechanisms, which allows to convert the absorbed light energy into reorientation energy. The first time, it is reported an experimental study of the optical properties dynamics of the hybrid alignment of nematic liquid crystal (NLC) under the influence of flow caused by volume expansion mechanism [15]. In this paper it is presented initially hybrid-oriented LC, which is affected by a laser light. Laser-induced hydrodynamic motions change the orientation of the LC. It is discussed some cases of reorientation using different power of laser. It is useful to know the laser power which is able to make reorientation of LC molecules. Here we also take into account the anchoring energies which play a big role in our study.

2. ANCHORING ENERGY AND REORIENTATION

LC molecules are not fully oriented in the absence of external influences but preferably oriented only within small domains. For the LC to be homogeneously oriented throughout the cell, it is necessary to give certain boundary conditions to the walls of the LC. Anchoring energy is involved in boundary conditions. In this paper we describe the reorientation induced by direct volume expansion. This mechanism is introduced in some papers [7, 15, 16]. The LC cell is connected with another LC volume (FIGURE 1), which is designed for absorbing the light energy. That creates a volume expansion and becomes the reason of hydrodynamic flow, because the expansion of the liquid creates a pressure gradient over the cell. We assume that the pressure gradient is along the x-axis, resulting in a Poiseuille flow [17] with $\mathbf{v} = v\mathbf{e}_x$, where \mathbf{v} is the velocity of hydrodynamic flow in the cell. We consider $\partial/\partial x = \partial/\partial y = 0$ and the director \mathbf{n} stays in (x,z) plane. Then the equation of the reorientation angle $\varphi(z, t)$ can be deduced considering NLC director reorientation, Navier-Stokes and thermal conductivity equations which describe our system [7]:

$$\begin{aligned} & \left(\frac{\partial\varphi}{\partial z}\right)^2 \sin\varphi \cos\varphi (K_1 - K_3) + \frac{\partial^2\varphi}{\partial z^2} (K_3 \cos^2\varphi + K_1 \sin^2\varphi) = \\ & = \frac{6\beta\chi V}{\rho c_p l L^3} P(2z - L)(\alpha_2 \cos^2\varphi - \alpha_3 \sin^2\varphi) + \frac{\partial\varphi}{\partial t} (\alpha_3 - \alpha_2) \end{aligned} \quad (1)$$

where φ is the reorientation angle, K_i are Frank's elastic constants, α_i are Leslie coefficient of NLC, ρc_p is the specific volume thermal capacitance (in erg/cm^3K), χ is the absorption factor (in cm^{-1})

and P is the laser radiation power (in erg/cm^3), V is the volume of absorbing liquid and β is the thermal expansion coefficient (in K^{-1}).

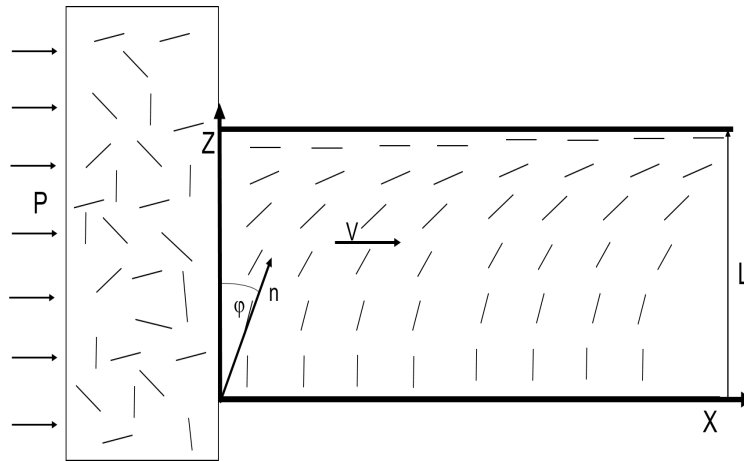


Figure 1: Schematic representation of direct volume expansion mechanism.

From mathematical point of view, it is more suitable to write this equation in the following form:

$$\frac{\partial \varphi}{\partial \tau} = K + (\Delta \sin^2 \varphi) \frac{\partial^2 \varphi}{\partial \zeta^2} + \frac{1}{2} \sin 2\varphi \left(\frac{\partial \varphi}{\partial \zeta} \right)^2 + DP(2\zeta - 1)(\alpha \sin^2 \varphi - 1) \quad (2)$$

where the following notations are done: $K = K_3/K_1$, $\Delta = (K_1 - K_3)/K_1$, $\alpha = (\alpha_3 + \alpha_2)/\alpha_2$, $\zeta = z/L$, $\tau = K_1 t / (\gamma L^2)$, $\gamma = \alpha_3 - \alpha_2$, $D = 6\beta\chi V\alpha_2 / (K_1 \rho c_\rho)$.

Equation (2) describes a laser-induced (without threshold) hydrodynamic flow in an NLC with the director confined in the (x, z) plane. We are going to solve this equation using "Mathematica". Nevertheless, we need to define the boundary and the initial conditions in order to be able to solve the equation. The boundary conditions are related to the anchoring energies.

There are some articles about the measurement of anchoring energies. It is suggested a way to evaluate the anchoring energy of LC by determining the LC tilt angle at the boundary of a substrate. There is explained the theory how to calculate it and also some experimental results [18]. The experimental measurement of anchoring energy strength of LC cells is described in their work [19]. The technique is based on the possibility of gathering a large amount of very precise data about the linear optical response of the cell in different experimental conditions, using spectroscopic ellipsometry. In our article we discuss hybrid-oriented NLC. Which means the initial condition can be written by the following form:

$$\varphi(0, \zeta) = \frac{\pi}{2} \zeta \quad (3)$$

this means that on the lower wall we have homeotropic orientation and on the upper wall the molecules are planar-oriented.

As we study the influence of anchoring energies on the reorientation, they must be represented on boundary conditions. In other words we define the boundary conditions which depend on anchoring energies. The values of the latter are in this range: $10^{-4} - 10^{-1} erg/cm^2$ [18]. If the anchoring energy

is 10^{-1}erg/cm^2 the boundary condition is strong, means there is no change of orientation on the boundary. For hybrid-orientated LC the boundary conditions have the following form corresponding for the lower ($z=0$) and the upper($z=L$) walls:

$$(K_1 \sin^2 \varphi + K_3 \cos^2 \varphi) \frac{\partial \varphi}{\partial z} - \sigma_1 \sin \varphi \cos \varphi = 0 \quad (4)$$

$$(K_1 \sin^2 \varphi + K_3 \cos^2 \varphi) \frac{\partial \varphi}{\partial z} - \sigma_2 \sin \varphi \cos \varphi = 0 \quad (5)$$

In the above equations, σ_1 and σ_2 are the coefficients of surface anchoring energy (in erg/cm^2). The NLC can be considered as a "flexible ribbon" due to its elasticity. We have studied 2 directions of hydrodynamic flow (FIGURE 2).

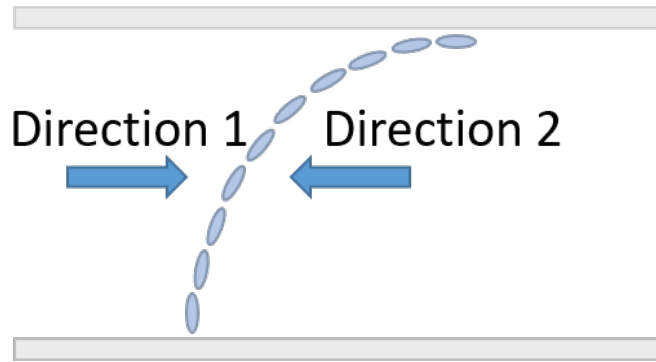


Figure 2: Representation of the LC as a "flexible ribbon". Direction 1 and 2 are the directions of the hydrodynamic flow.

3. NUMERICAL SOLUTIONS AND DISCUSSION

Equation (2) was solved for 2 directions of hydrodynamic flow with Eq. (3-5) initial and boundary conditions using "Mathematica-11". In the calculation for NLC MBBA [20] we assumed $K_1 = 10^{-6} \text{erg/cm}$, $K_3 = 7.5 \cdot 10^{-7} \text{erg/cm}$, $\alpha_2 = 0.8P$, $\alpha_3 = 0.012P$, $\beta = 10^{-3} K^{-1}$, $\rho c_\rho = 1J/cm^3 K$, $V = 1cm^3$, $L = 12\mu m$, $l = 0.1cm$. NLC MBBA and geometrical sizes of the cell we choose as an example. The hydrodynamic flow velocity and director reorientation arises without light intensity threshold and decreases with increasing of cell thickness. In this paper we have studied the reorientation induced by different laser power.

In the case of the first direction of hydrodynamic flow we get totally different results when we change the boundary conditions. When the surface anchoring energy of the lower wall (initially homeotropic-oriented wall) is 10^{-3}erg/cm^2 (weak boundary condition), and the energy of the upper wall (initially planar-oriented) is 10^{-1}erg/cm^2 (strong boundary condition), hydrodynamic flow tries to make the molecules to take the direction of the flow [20]. In Fig. 3(a) it is presented how the reorientation induced by different laser power is changed 0.9 seconds after the start of the hydrodynamic flow. 0.9 seconds is the time after which there is no more reorientation in the case of $0.5mW/cm^3$ laser power. We can see that weak laser light ($0.05mW/cm^3$) almost do not change the

orientation and $0.5mW/cm^3$ laser power is enough to reorient the molecules to planar, but is much weaker than that is necessary for NLC phase transition. It is important, also, that light is absorbed by big volume (left side in the FIGURE 1) and the reorientation happens in the thin LC cell. It means that even for higher light intensity absorption and phase transition in the big volume will not affect on the phase transition in the thin cell for long time period. If the power is higher than $0.5mW/cm^3$ the reorientation takes place rapidly and the reorientation angle becomes larger. This is easy to see in Fig. 3(b), where is shown the change of the reorientation angle along the cell and in time under $1mW/cm^3$ laser radiation. In addition, as much the surface anchoring energy of the lower wall is smaller, the reorientation angle of the molecules near the lower wall is greater.

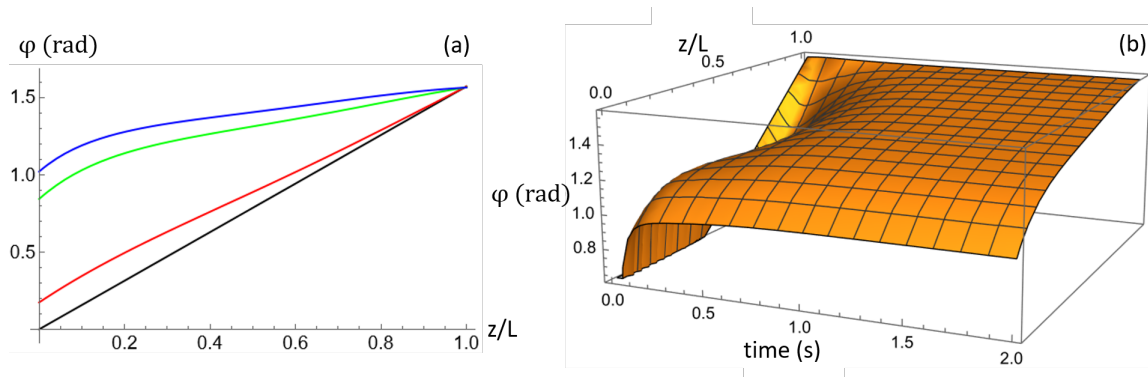


Figure 3: The reorientation angle when it is applied weak boundary condition to the lower and strong boundary condition to the upper wall. a) The angle between the director and z axis for different laser power: The black line corresponds to the initial state ($T = 0$ s, no reorientation). The colored curves correspond to reorientation caused 0.9 s after launching the laser radiation. Red: $P=0.05mW/cm^3$, green: $P=0.5mW/cm^3$, blue: $P = 1mW/cm^3$. b) The change of the reorientation angle along the cell and in time at $1mW/cm^3$ fixed power.

When the surface anchoring energy of the lower wall is $10^{-1}erg/cm^2$, and the energy of the upper wall is $10^{-3}erg/cm^2$, the “flexible ribbon” reverses its curvature Fig. 4. It takes place at the time when deformation energy becomes larger than surface anchoring energy. When the curvature is reversed hydrodynamic flow is directed already out of it and we detect an additional increase of curvature.

In this case if we take the value of the laser power $0.05 mW/cm^3$, then the reorientation occurs gradually, the reorientation angle decreases and the reorientation dependence on z/L is close to linear dependence and there is no reversing of curvature. When the laser power is higher ($4mW/cm^3$) the reversing of curvature is more obvious and emerges faster. In FIGURE 4(b) it is shown the change of the reorientation angle along the cell and in time under $4mW/cm^3$ laser radiation.

In the case of the second direction, when the flow velocity is directed out of the “flexible ribbon’s” curvature, the curvature increases [20]. In FIGURE5(a) and FIGURE6(a) is presented how the reorientation induced by different laser power is changed respectively 0.5 and 0.7 s after the start of the hydrodynamic flow. Those are the required time periods for the molecules to take their final reorientation under $0.5mW/cm^3$ laser radiation. We have observed different switching

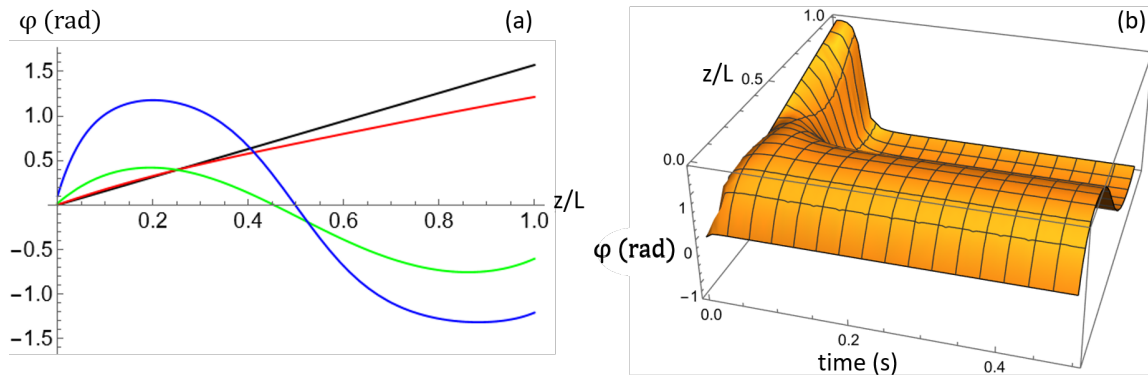


Figure 4: The reorientation angle when it is applied strong boundary condition to the lower and weak boundary condition to the upper wall. a) The angle between the director and z axis for different laser power: The black line corresponds to the initial state ($T = 0$ s, no reorientation). The colored curves correspond to reorientation caused 1 s launching the laser radiation. Red: $P=0.05 \text{ mW/cm}^3$, green: $P=0.5 \text{ mW/cm}^3$, blue: $P = 4 \text{ mW/cm}^3$. b) The change of the reorientation angle along the cell and in time at 4 mW/cm^3 fixed power.

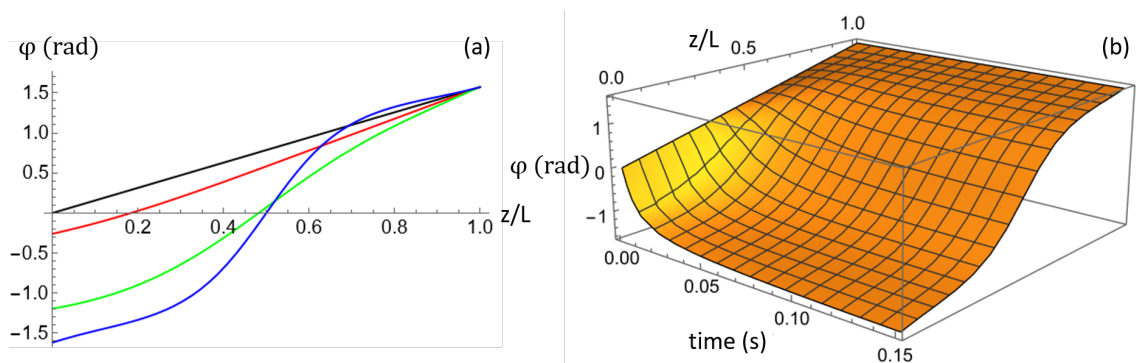


Figure 5: The reorientation angle when it is applied weak boundary condition to the lower and strong boundary condition to the upper wall. a) The angle between the director and z axis for different laser power: The black line corresponds to the initial state ($T = 0$ s, no reorientation). The colored curves correspond to reorientation caused 0.5 s after launching the laser radiation. Red: $P=0.05 \text{ mW/cm}^3$, green: $P=0.5 \text{ mW/cm}^3$, blue: $P = 4 \text{ mW/cm}^3$. b) The change of the reorientation angle along the cell and in time at 4 mW/cm^3 fixed power.

times since the boundary conditions are different and the LC reorientation behaves differently depends on the direction of hydrodynamic flow. When we have small anchoring energy at the lower wall, the orientation of the molecules near that wall is changed (FIGURE 5(a)). When we have small anchoring energy at the upper wall, where the molecules are initially planar-oriented, the hydrodynamic flow almost doesn't change the orientation of the molecules (FIGURE 6(a)). The

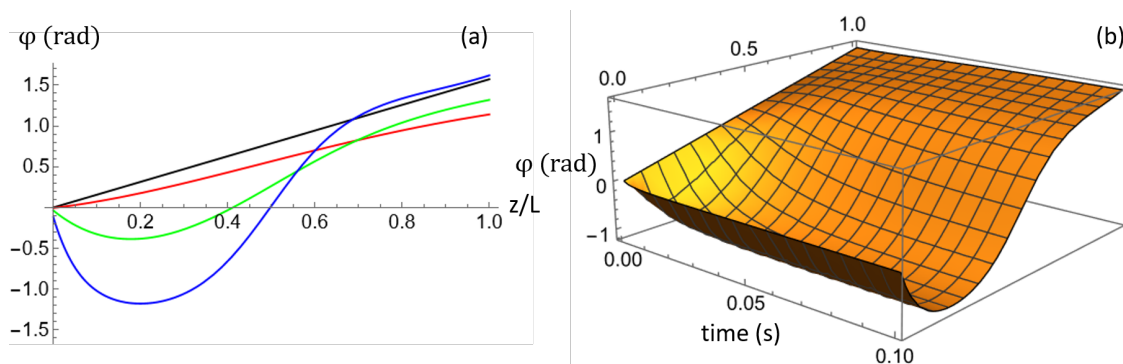


Figure 6: The reorientation angle when it is applied strong boundary condition to the lower and weak boundary condition to the upper wall. a) The angle between the director and z axis for different laser power: The black line corresponds to the initial state ($T = 0$ s, no reorientation). The colored curves correspond to reorientation caused 0.7 s after launching the laser radiation. Red: $P = 0.05 \text{ mW/cm}^3$, green: $P = 0.5 \text{ mW/cm}^3$, blue: $P = 4 \text{ mW/cm}^3$. b) The change of the reorientation angle along the cell and in time at 4 mW/cm^3 fixed power.

study of the reorientation due to the absorption of 0.05 mW/cm^3 laser shows that the reorientation occurs slowly and the angle of reorientation decreases. In the case of high power 4 mW/cm^3 the curvature becomes bigger and the reorientation occurs faster (FIGURE5(b) and FIGURE 6(b)). In the second direction of the hydrodynamic flow, planar-oriented molecules almost do not change their orientation and remain planar even when the surface anchoring energy is 10^{-4} erg/cm^2 . This is because planar-oriented molecules have flow direction which is considered as a preferable direction for the molecules.

4. CONCLUSION

In this paper it is presented initially hybrid-oriented LC and it is discussed some cases of reorientation using different laser power. We have studied the difference of molecules reorientation depend on boundary conditions. Let us present hybrid initial orientation of nematic liquid crystal cell as “flexible ribbon”. We revealed that there is no curvature reversing in the case when the hydrodynamic flow is directed out of the “flexible ribbon’s” curvature and the laser power is too weak, the flow brings an increase of the curvature. The curvature deforms more completely and the deformation increases in time when velocity is directed into “flexible ribbon’s” curvature. The deformation free energy initially increases until saturation. The “flexible ribbon” reverses its curvature at the time when deformation energy becomes larger than surface anchoring energy at the wall with planar initial orientation, and takes a form with less deformation energy. In that way hydrodynamic velocity is directed out of the reversed curvature and brings an additional small increase of curvature. The reversing time depends on NLC parameters and surface coupling energy. The latter depends on the method of surface treatment. Higher intensities make the process of reorientation faster. The development of this concept and implementation could also be a new indirect way of measuring anchoring energies of NLC. We have to note that in our case a) laser-induced hydrodynamic flow

has no threshold by light intensity, b) the light wavelength is related only in terms of absorption and was not used in calculations, c) calculations are general for all NLC.

Funding. The work was supported by the Science Committee of the Republic of Armenia in the frames of research project 21AG-1C088.

Disclosures. The authors declare no conflicts of interest.

References

- [1] Kim YK, Senyuk B, Lavrentovich OD. Molecular Reorientation of a Nematic Liquid Crystal by Thermal Expansion. *Nat Commun.* 2012;3:1133.
- [2] Akopyan RS, Zel'dovich BY. Reorientation of Liquid-Crystal Director by Light Near the Thresh-Old of Spatially Periodic Convective Instability. *Zh Eksp Teor Fiz.* 1984;86:533-544.
- [3] Tabiryan NV, Sukhov AV, Zel'Dovich BY. Orientational Optical Nonlinearity of Liquid Crystals. *Mol Cryst Liq Cryst.* 1986;136:1-39.
- [4] Akopyan RS, Tabiryan NV, Tschudi T. Optically Induced Hydrodynamic Reorientation of Liquid Crystals and Its Applications for Infrared Detection and Information Storage. *Phys Rev E.* 1994;49:3143.
- [5] Hakobyan RS, Zeldovich BY. Excitation of Surface Capillary Waves by Spatially Periodical Laser Radiation. *J Nonlinear Optic Phys Mat.* 2004;13:1-6.
- [6] Nys I. Patterned Surface Alignment to Create Complex Three-Dimensional Nematic and Chiral Nematic Liquid Crystal Structures. *Liq Cryst Today.* 2020;29:65-83.
- [7] Hakobyan RS, Sargsyan KM, Tabirian NV. Jump-Like Light-Induced Hydrodynamicreorientation of Lc's Caused by Direct Volume Expansion. *Mol Cryst Liq Cryst.* 2006;453:239-250.
- [8] Zel'dovich BY, Tabiryan N. Interaction of light waves with nonuniformly oriented liquid crystals, *Opt. eff. Liq Cryst.* 1986:165-171.
- [9] Sharma M, Sharma M, Ellenbogen T. An All Optically Liquid Crystal Plasmonic Metasurface Platform. *Laser Photonics Rev.* 2020;14:2000253.
- [10] Di Pietro VM, Jullien A, Bortolozzo U, Forget N, Residori S, et al. Thermally Induced Non-linear Spatial Shaping of Infrared Femtosecond Pulses in Nematic Liquid Crystals. *Laser Phys Lett.* 2018;16:015301.
- [11] Zakharov A, Vakulenko A. Influence of the Flow on the Orientational Dynamics Induced by Temperature Gradient in Nematic Hybrid-Oriented Cells. *J Chem Phys.* 2007;127:084907.
- [12] Zakharov AV, Vakulenko AA. Orientational Nematodynamics of a Hybrid-Oriented Capillary. *Phys Solid State.* 2010;52:1542-1548.
- [13] Škarabot M, Maček Kržmanc M, Rupnik L, Lahajnar G, Suvorov D, et al. Electric-Field-Induced Reorientation of Ferroelectric Micro- And Nanoplatelets in the Nematic Liquid Crystal. *Liq Cryst.* 2021;48:385-394.

- [14] Lucchetti L, Kushnir K, Reshetnyak V, Ciciulla F, Zaltron A, et al. Light-Induced Electric Field Generated by Photovoltaic Substrates Investigated Through Liquid Crystal Reorientation. *Opt Mater.* 2017;73:64-69.
- [15] Dadalyan T, Petrosyan K, Alaverdyan R, Hakobyan R. Light-Induced Hydrodynamic Reorientation of Hybrid Aligned Nematic Liquid Crystals Caused by Direct Volume Expansion. *Liq Cryst.* 2019;46:694-699.
- [16] Hakobyan M, Alaverdyan R, Hakobyan R, Chilingaryan YS. Volume Expansion Mechanism of Laser-Induced Hydrodynamic Reorientation. *Armen. J Phys.* 2014;7.
- [17] Pfitzner J. Poiseuille and His Law. *Anaesthesia.* 1976;31:273-275.
- [18] Rivière D, Lévy Y, Guyon E. Determination of Anchoring Energies From Surface Til Tangle Measurements in a Nematic Liquid Crystal. *J Phys Lettres.* 1979;40:215-218.
- [19] Marino A, Tkachenko V, Santamato E, Bennis N, Quintana X, et al. Measuring Liquid Crystal Anchoring Energy Strength by Spectroscopic Ellipsometry. *J Appl Phys.* 2010;107:073109.
- [20] Fernandes PRG, da Silva KA, Mukai H, Muniz EC. Optical, Morphological and Dielectric Characterization of Mbba Liquid Crystal-Doped Hydrogels. *J Mol Liq.* 2017;229:319-329.